**ARSET**

Applied Remote Sensing Training

http://arset.gsfc.nasa.gov

@NASAARSET

# Introduction to SAR Interferometry

Eric Fielding

Jet Propulsion Laboratory

# Learning Objectives

By the end of this presentation, you will be able to:

- Understand the basic physics of SAR interferometry
- Describe what SAR interferometric phase tells about the land surface
- Describe the necessary data preprocessing
- Understand the information content in SAR interferometric images
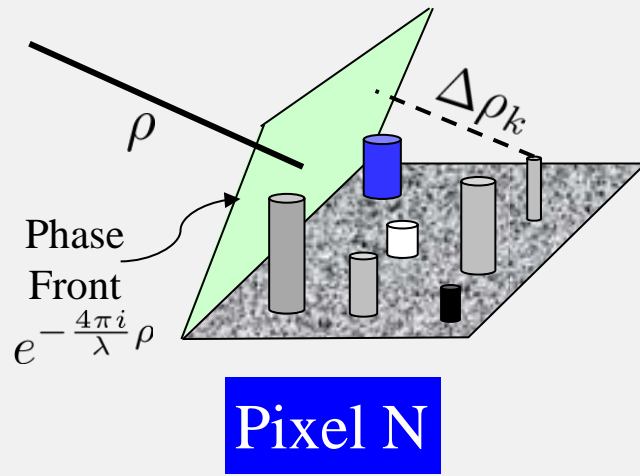
# Prerequisites

- Basics of Synthetic Aperture Radar
- SAR Processing and Data Analysis

# SAR Interferometry Theory

# SAR Imagery and Speckle

- Full resolution SAR imagery has a grainy appearance called speckle, which is a phenomena due to the coherent nature of SAR imaging.

$\rho$

$\Delta\rho_k$

Phase
Front
$e^{-\frac{4\pi i}{\lambda}\rho}$

Pixel N

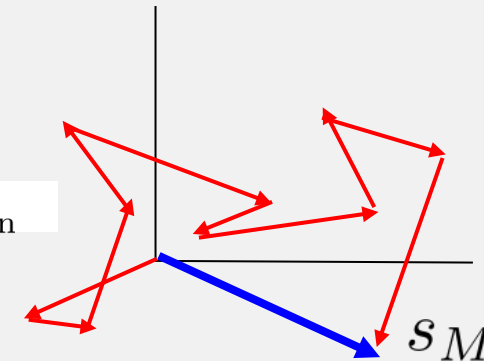Number and arrangement of scattering elements within resolution cell varies from pixel to pixel.

Returned signal is a coherent combination of the returns from the scattering elements.
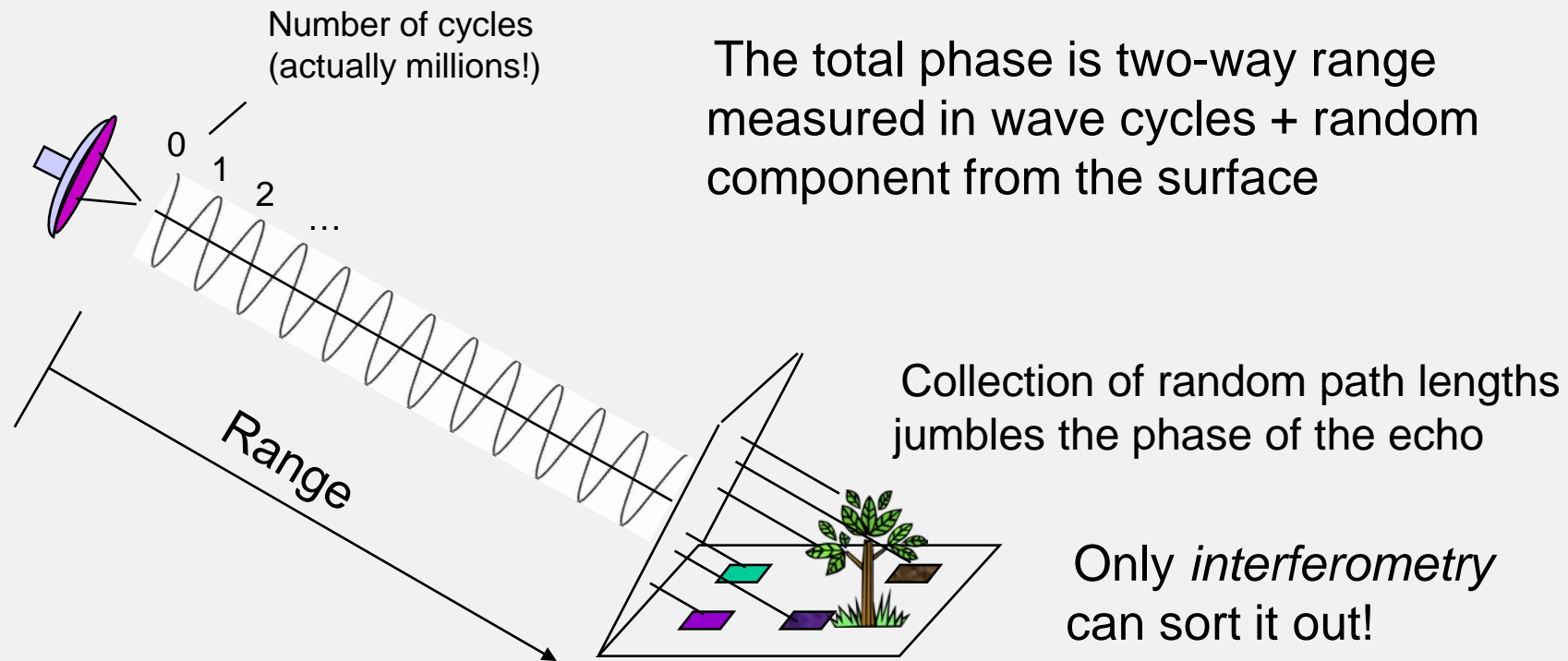
Pixel M
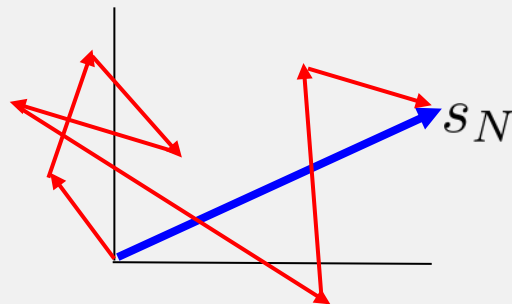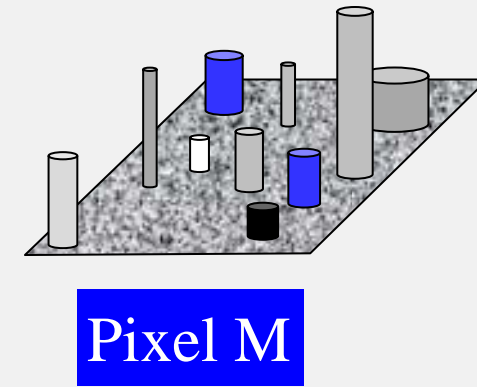
$$s = A \underbrace{e^{-\frac{4\pi i}{\lambda}\rho}}_{\text{Range Phase}} \underbrace{\sum_{k=1}^{N} a_k e^{-\frac{4\pi i}{\lambda}\Delta\rho_k}}_{\text{Scatterer Contribution}}$$

$s_N$

$s_M$

Slide Courtesy of Paul Rosen (JPL)

# SAR Phase - A Measure of the Range and Surface Complexity

The phase of the radar signal is the number of *cycles of oscillation* that the wave executes between the radar and the surface and back again.

Number of cycles
(actually millions!)

0
1
2
...

Range

The total phase is two-way range measured in wave cycles + random component from the surface

Collection of random path lengths jumbles the phase of the echo

Only *interferometry* can sort it out!

Slide Courtesy of Paul Rosen (JPL)

# Simplistic view of SAR phase

Phase of image 1

$$\phi_1 = \frac{4\pi}{\lambda} \cdot \rho_1 + \text{other constants} + n_1$$

Phase of image 2

$$\phi_2 = \frac{4\pi}{\lambda} \cdot \rho_2 + \text{other constants} + n_2$$

1. The "other constants" cannot be directly determined.

2. "Other constants" depends on scatterer distribution in the resolution cell, which is unknown and varies from cell to cell.

3. Only way of observing the range change is through interferometry (cancellation of "other constants").

Slide modified from Paul Rosen (JPL)
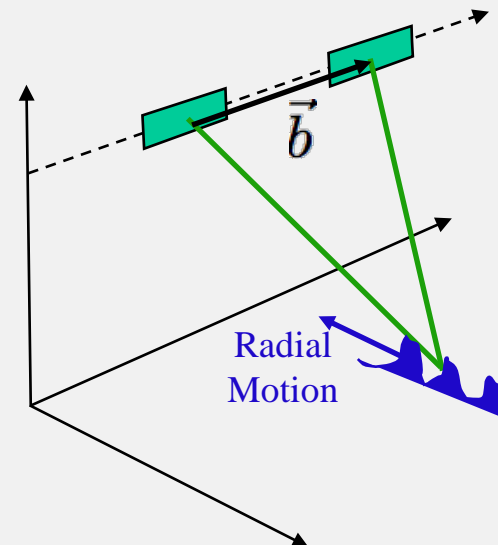
# Types of Radar Interferometry

- Two main classes of interferometric radars are separated based on the geometric configuration of the baseline vector:

  – Interferometers are used for topographic measurements when the antennas are separated in the cross-track direction.

  – Interferometers are used to measure line-of-sight motion when the antennas are separated in the along-track direction.

  – A single antenna repeating its path can form an interferometer to measure long-term deformation

## Cross-Track Interferometer

## Along-Track Interferometer
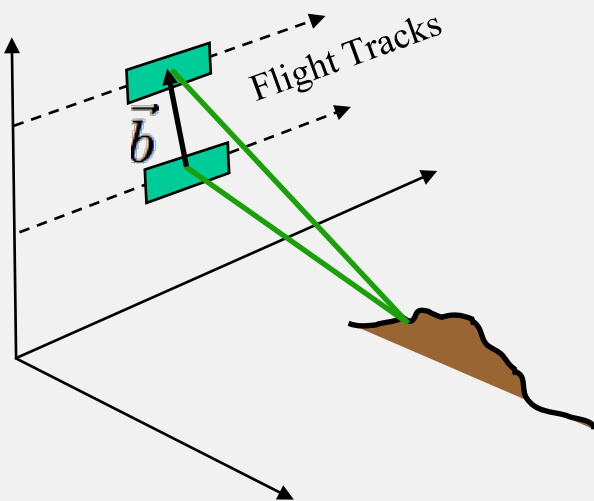
- Dual antenna single pass interferometers
- Single antenna repeat pass interferometers
  ==> Topography and Deformation

- Dual antenna single pass interferometer
- Along-track separation
  ==> Radial velocity

Slide modified from Paul Rosen (JPL)

# SAR Interferometry Applications

- Mapping/Cartography
  - Radar Interferometry from airborne platforms is routinely used to produce topographic maps as digital elevation models (DEMs).
    - 2-5 meter circular position accuracy
    - 5-10 m post spacing and resolution
    - 10 km by 80 km DEMs produced in 1 hr on mini-supercomputer
  - Radar imagery is automatically geocoded, becoming easily combined with other (multispectral) data sets.
  - Applications of topography enabled by interferometric rapid mapping
    - Land use management, classification, hazard assessment, intelligence, urban planning, short and long time scale geology, hydrology
- Deformation Mapping and Change Detection
  - Repeat Pass Radar Interferometry from spaceborne platforms is routinely used to produce topographic *change* maps as digital displacement models (DDMs).
    - 0.3-1 centimeter relative displacement accuracy
    - 10-100 m post spacing and resolution
    - 100 km by 100 km DDMs produced rapidly once data is available
  - Applications include
    - Earthquake and volcano monitoring and modeling, landslides and subsidence
    - Glacier and ice sheet dynamics
    - Deforestation, change detection, disaster monitoring

Slide modified from Paul Rosen (JPL)

# Interferometry for Topography

Measured phase difference:

$$\otimes\phi = -\frac{2\pi}{\lambda}\delta\rho$$
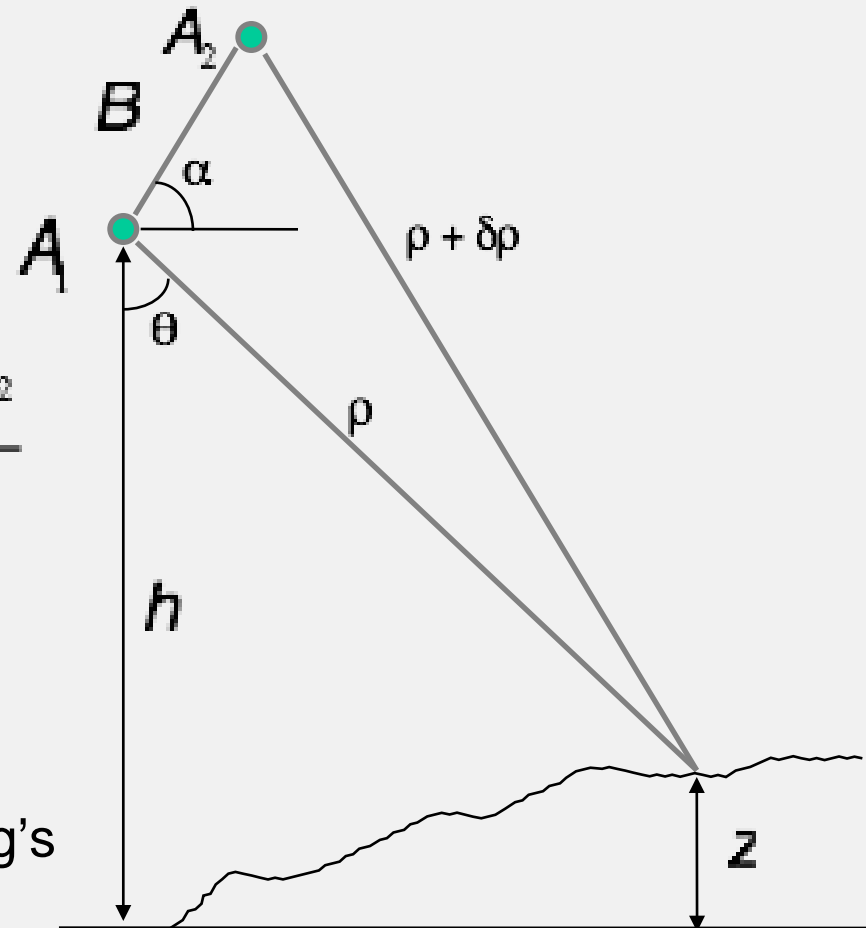
Triangulation:

$$\sin(\theta - \alpha) = \frac{(\rho + \delta\rho)^2 - \rho^2 - B^2}{2\rho B}$$

$$z = h - \rho\cos\theta$$

Critical Interferometer Knowledge:
- Baseline, $(B, \alpha)$ to mm's
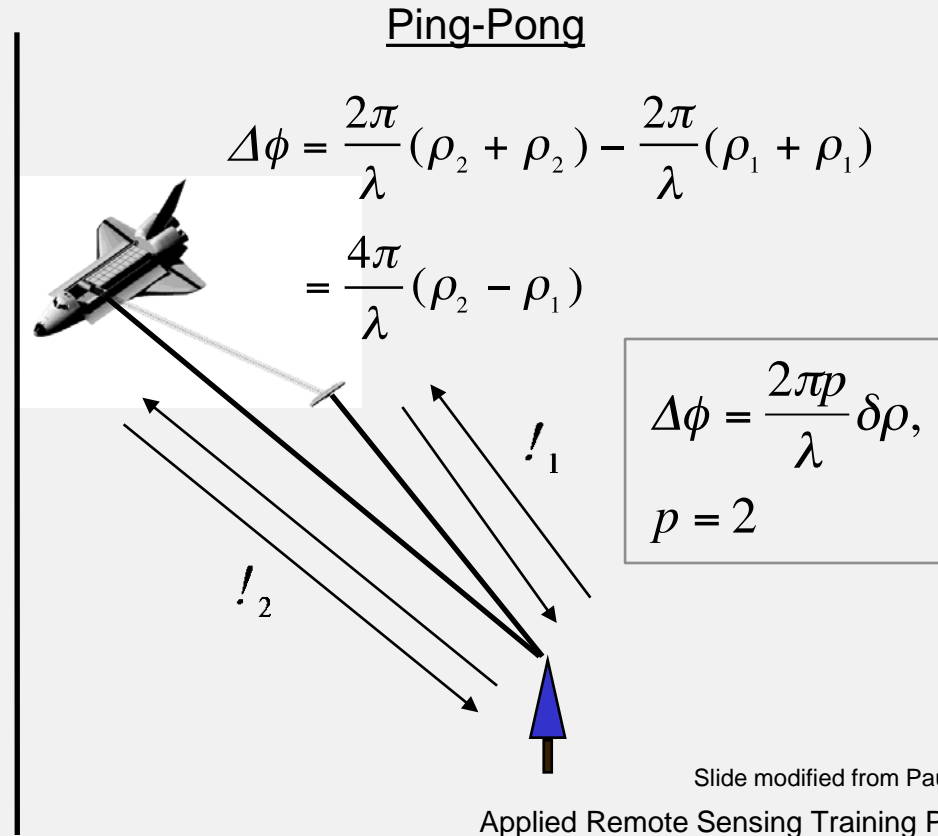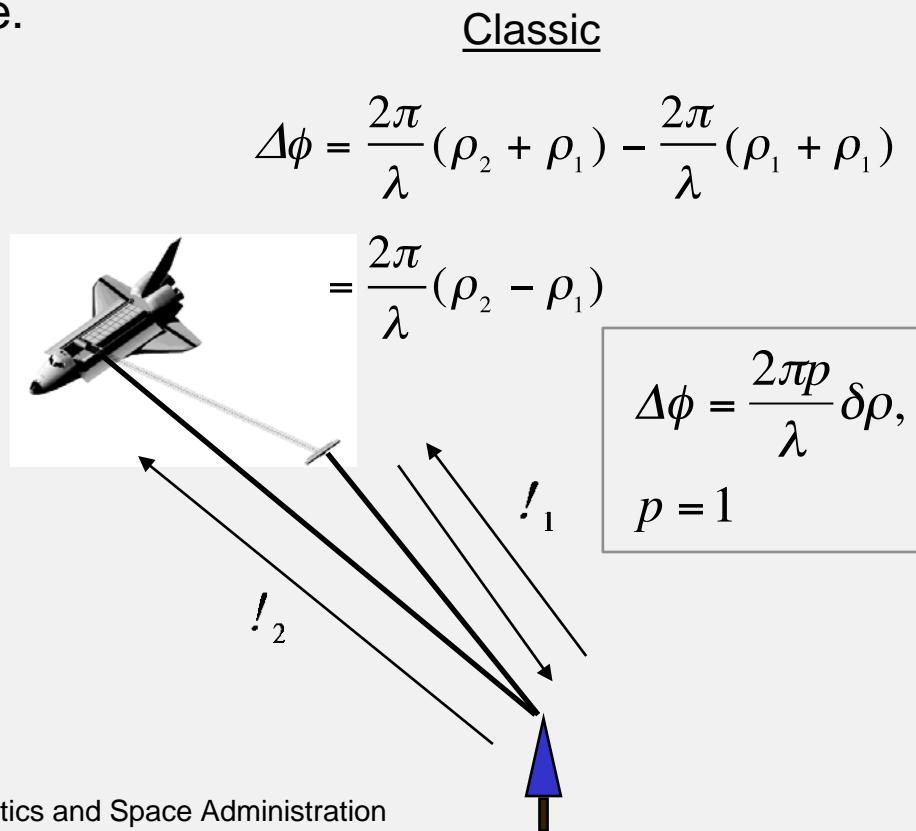- System phase differences, to deg's

# Data Collection Options

For single pass interferometry (SPI) both antennas are located on the same platform, which is ideal for measuring topography. Two modes of data collection are common:
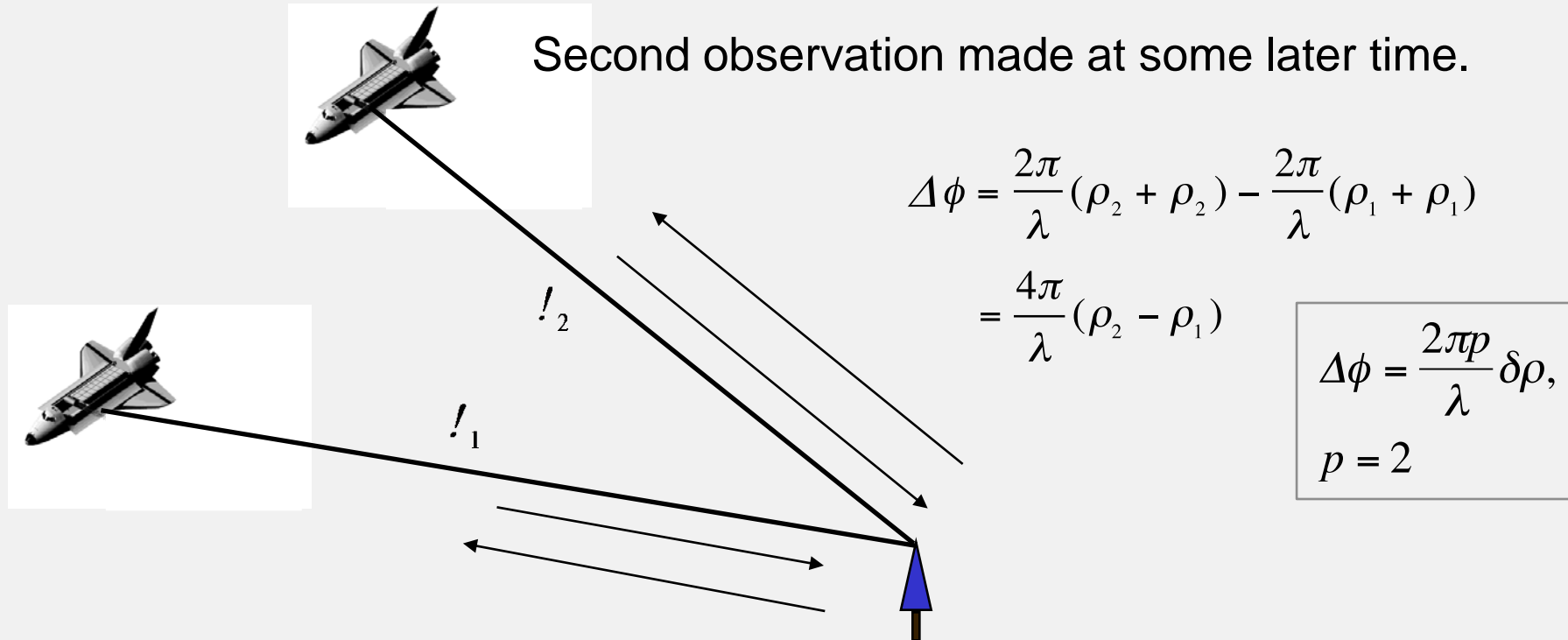
- *single-antenna-transmit mode* - one antenna transmits and both receive
- *ping-pong mode* - each antenna transmits and receives its own echoes effectively doubling the physical baseline.

## Classic

$$\Delta\phi = \frac{2\pi}{\lambda}(\rho_2 + \rho_1) - \frac{2\pi}{\lambda}(\rho_1 + \rho_1)$$

$$= \frac{2\pi}{\lambda}(\rho_2 - \rho_1)$$

$$\Delta\phi = \frac{2\pi p}{\lambda}\delta\rho,$$

$$p = 1$$

## Ping-Pong

$$\Delta\phi = \frac{2\pi}{\lambda}(\rho_2 + \rho_2) - \frac{2\pi}{\lambda}(\rho_1 + \rho_1)$$

$$= \frac{4\pi}{\lambda}(\rho_2 - \rho_1)$$

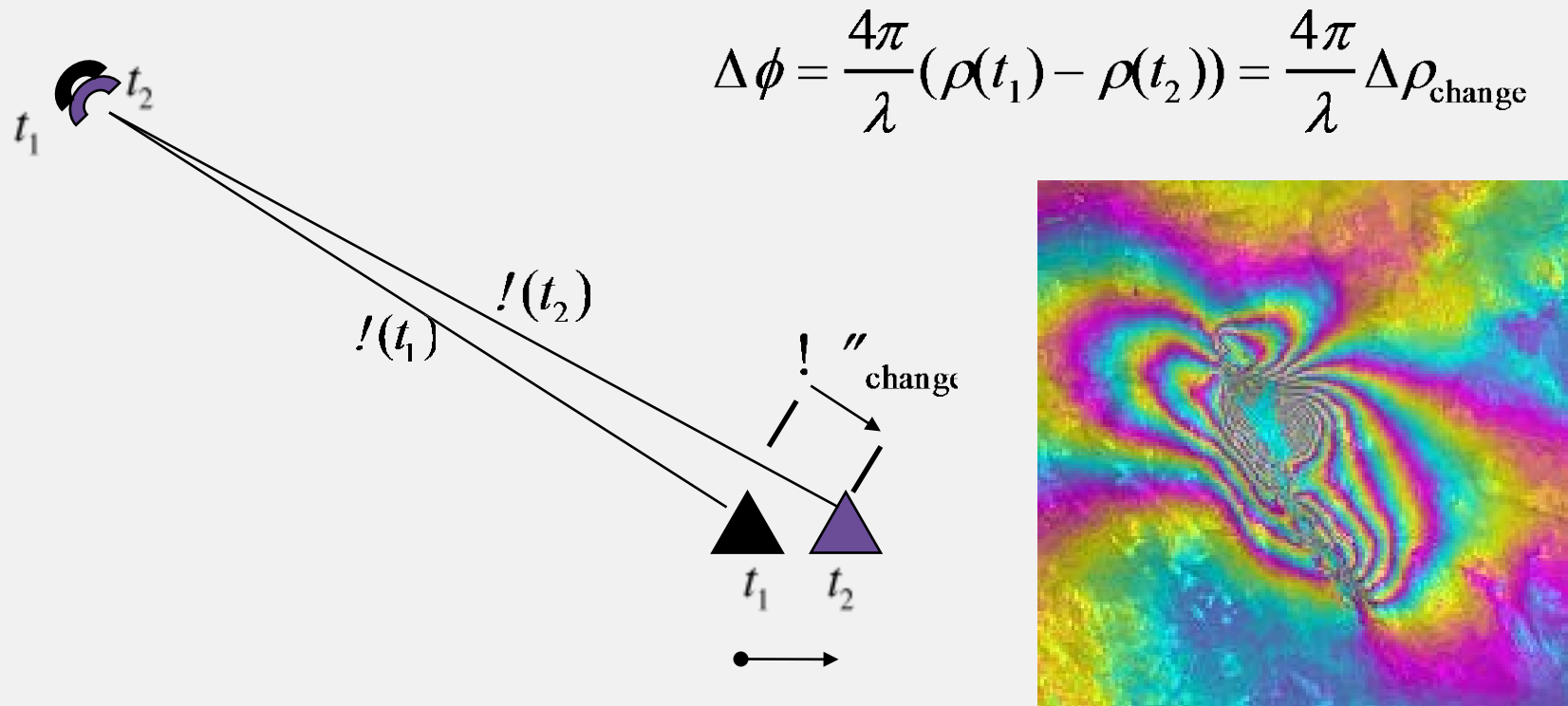$$\Delta\phi = \frac{2\pi p}{\lambda}\delta\rho,$$

$$p = 2$$

# Data Collection Options II

Interferometric data can also be collected in the repeat pass mode (RPI). In this mode two spatially close radar observations of the same scene are made separated in time. The time interval may range from seconds to years. The two observations may be made with different sensors provided they have nearly identical radar system parameters. This kind of data can be used for topography or surface deformation measurements.

Second observation made at some later time.

$$\Delta\phi = \frac{2\pi}{\lambda}(\rho_2 + \rho_2) - \frac{2\pi}{\lambda}(\rho_1 + \rho_1)$$

$$= \frac{4\pi}{\lambda}(\rho_2 - \rho_1)$$

$$\Delta\phi = \frac{2\pi p}{\lambda}\delta\rho,$$

$$p = 2$$

$\rho_2$

$\rho_1$

National Aeronautics and Space Administration

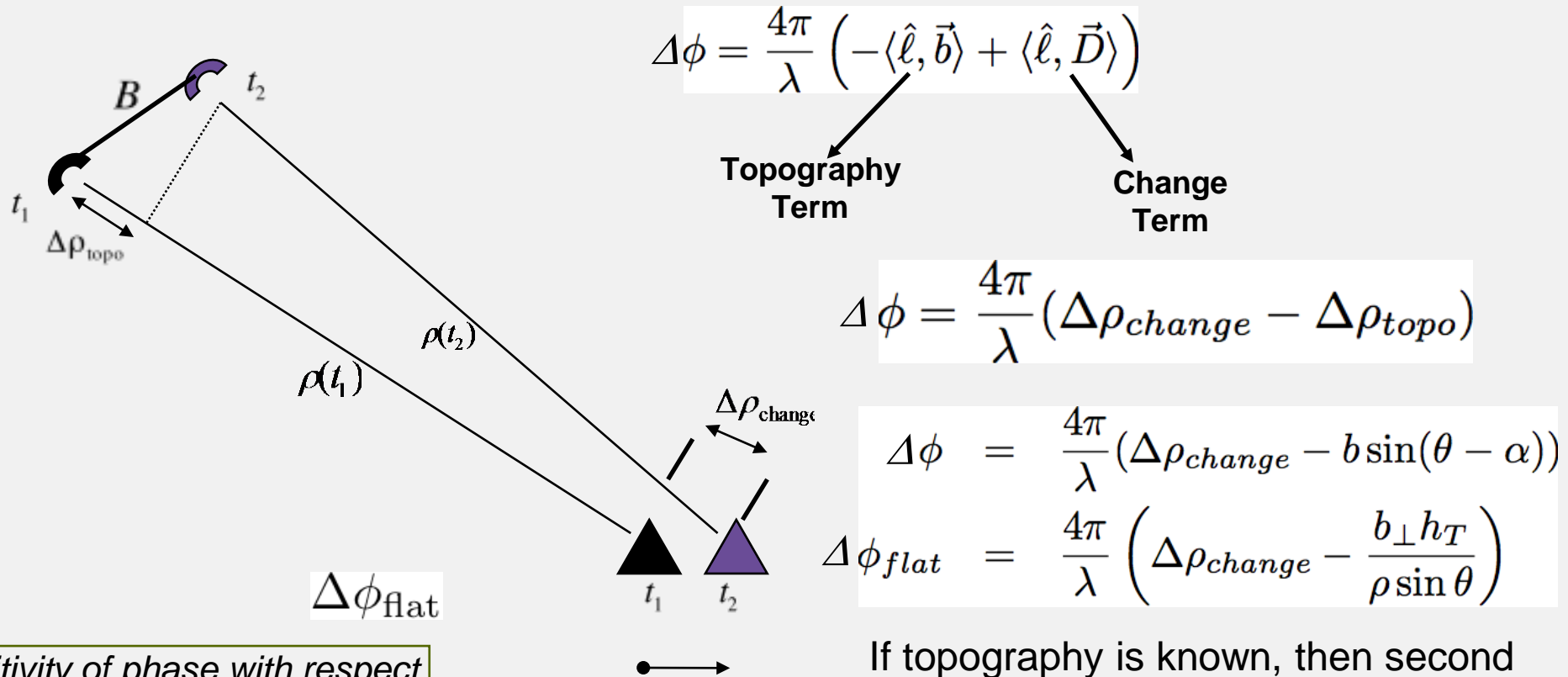Applied Remote Sensing Training Program

# Differential Interferometry

When two observations are made from the same location in space but at different times, the interferometric phase is proportional to any change in the range of a surface feature directly.

$$\Delta\phi = \frac{4\pi}{\lambda}(\rho(t_1) - \rho(t_2)) = \frac{4\pi}{\lambda}\Delta\rho_{\text{change}}$$

National Aeronautics and Space Administration

Applied Remote Sensing Training Program

# Differential Interferometry and Topography

- Generally two observations are made from different locations in space and at different times, so the interferometric phase is proportional to topography and topographic change.

$$\Delta\phi = \frac{4\pi}{\lambda}\left(-\langle\hat{\ell},\vec{b}\rangle + \langle\hat{\ell},\vec{D}\rangle\right)$$

**Topography Term**

**Change Term**

$$\Delta\phi = \frac{4\pi}{\lambda}\left(\Delta\rho_{change} - \Delta\rho_{topo}\right)$$

$$\Delta\phi = \frac{4\pi}{\lambda}\left(\Delta\rho_{change} - b\sin(\theta - \alpha)\right)$$

$$\Delta\phi_{flat} = \frac{4\pi}{\lambda}\left(\Delta\rho_{change} - \frac{b_{\perp}h_T}{\rho\sin\theta}\right)$$

If topography is known, then second term can be eliminated to reveal surface change

$B$

$t_2$

$t_1$

$\Delta\rho_{topo}$

$\rho(t_2)$

$\rho(t_1)$

$\Delta\rho_{change}$

$\Delta\phi_{flat}$

$t_1$

$t_2$

Note: Sensitivity of phase with respect to change is much greater than with respect to topographic relief

# Differential Interferometry Sensitivities

- The reason differential interferometry can detect millimeter level surface deformation is that the differential phase is much more sensitive to displacements than to topography.

$$\frac{\partial \phi}{\partial h} = \frac{2\pi pb \cos(\theta - \alpha)}{\lambda \rho \sin \theta} = \frac{2\pi pb_\perp}{\lambda \rho \sin \theta}$$

Topographic Sensitivity

$$(\phi \Leftrightarrow \Delta\phi)$$

$$\frac{\partial \phi}{\partial \Delta\rho} = \frac{4\pi}{\lambda}$$

Displacement Sensitivity

$$\sigma_{\phi_{topo}} = \frac{\partial \phi}{\partial h}\sigma_h = \frac{4\pi}{\lambda}\frac{b_\perp}{\rho \sin \theta}\sigma_h$$

Topographic Sensitivity Term

$$\sigma_{\phi_{disp}} = \frac{\partial \phi}{\partial \Delta\rho}\sigma_{\Delta\rho} = \frac{4\pi}{\lambda}\sigma_{\Delta\rho}$$

Displacement Sensitivity Term

Since $\frac{b}{\rho} \ll 1$ ==> $\frac{\sigma_{\phi_{disp}}}{\sigma_{\Delta\rho}} \gg \frac{\sigma_{\phi_{topo}}}{\sigma_h}$

Meter Scale Topography Measurement - Millimeter Scale Topographic Change

# Phase Unwrapping

From the measured, wrapped phase, unwrap the phase from some arbitrary starting location, then determine the proper $2\pi$ phase "ambiguity".

$$\Delta\phi_{topo} = \frac{2\pi p}{\lambda}\left(\rho_1 - \rho_2\right) = \frac{2\pi p}{\lambda}\vec{b}\bullet\vec{l}$$

$$\Delta\phi_{meas} = \text{mod}\left(\Delta\phi_{topo}, 2\pi\right)$$

$$\Delta\phi_{unwrap}(s,\rho) = \Delta\phi_{topo}(s,\rho) + \Delta\phi_{const}$$

$\vec{b}$

**Actual phase**

$\pi$

**Wrapped (measured) phase**

$\Delta\phi_{meas}$

**Typical unwrapped phase**

$\pi$

$-\pi$

$\Delta\phi_{unwrap}$

$\Delta\phi_{const}$

$\Delta\phi_{topo}$
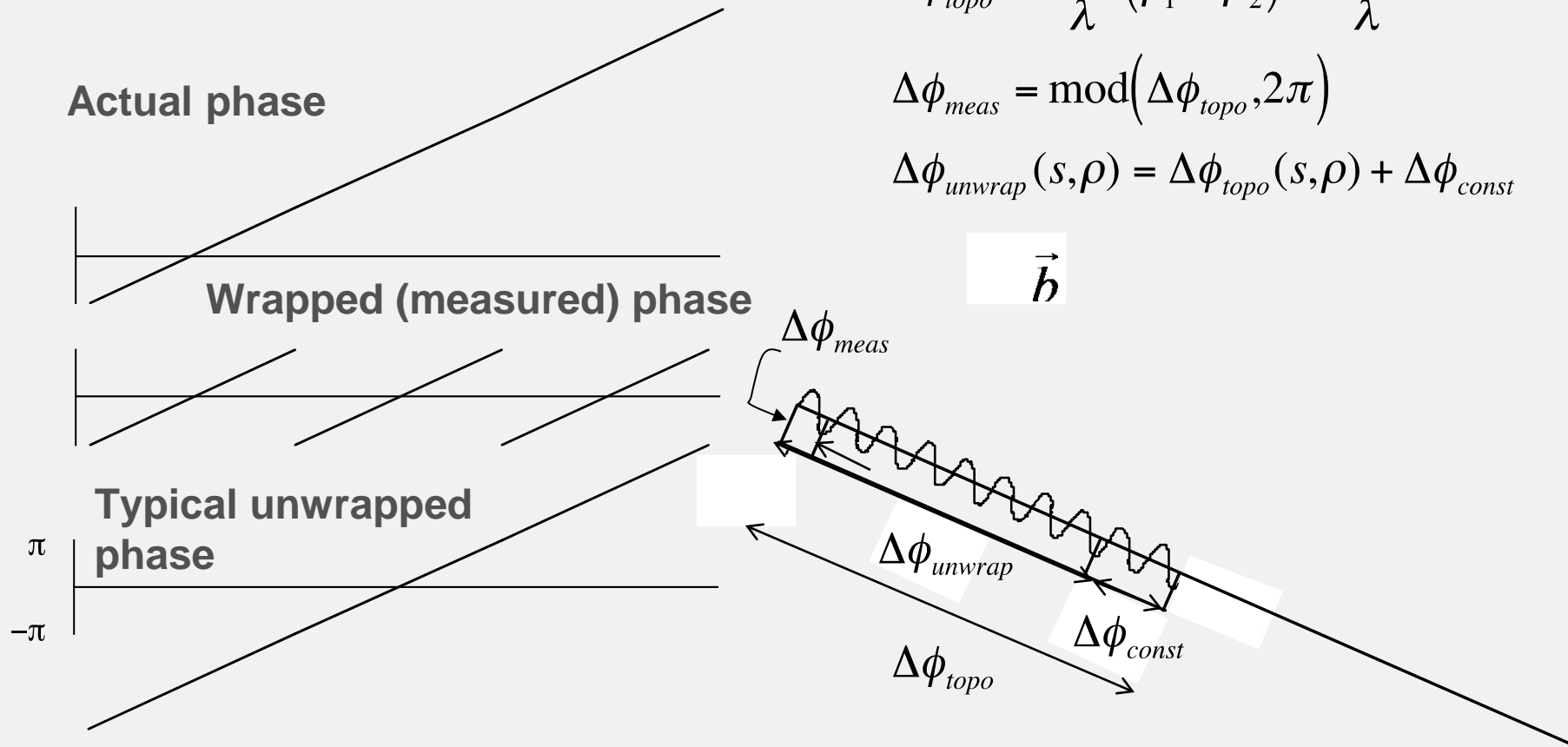
# Correlation* Theory

- InSAR signals decorrelate (become incoherent) due to

  - Thermal and Processor Noise

  - Differential Geometric and Volumetric Scattering

  - Rotation of Viewing Geometry

  - Random Motions Over Time

- Decorrelation relates to the local phase standard deviation of the interferogram phase

  - Affects height and displacement accuracy

  - Affects ability to unwrap phase

*"Correlation" and "Coherence" are often used synonymously

# InSAR correlation components

- Correlation effects multiply, unlike phase effects that add
- Low coherence or decorrelation for any reason causes loss of information in that area

$$\gamma = \gamma_v \gamma_g \gamma_t \gamma_c$$

where

$\gamma_v$ is volumetric (trees)

$\gamma_g$ is geometric (steep slopes)

$\gamma_t$ is temporal (gradual changes)

$\gamma_c$ is sudden changes

# InSAR Applications

# Some Examples of Deformation
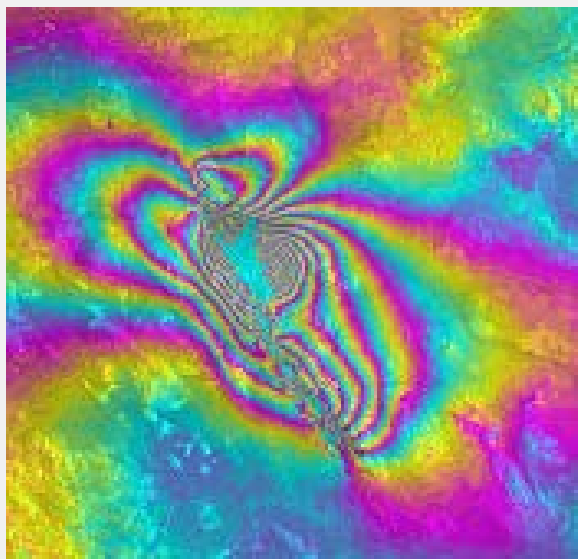


Hector Mine Earthquake

Etna Volcano

Ground subsidence near Pomona, California

Ice Velocities
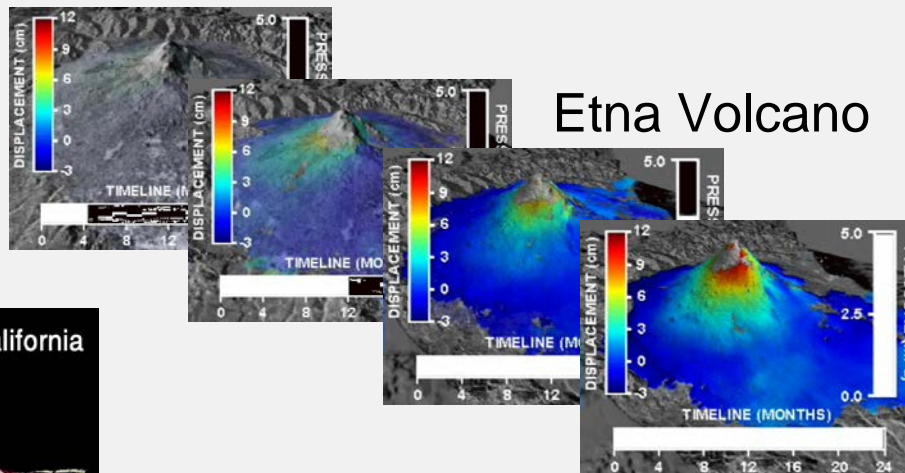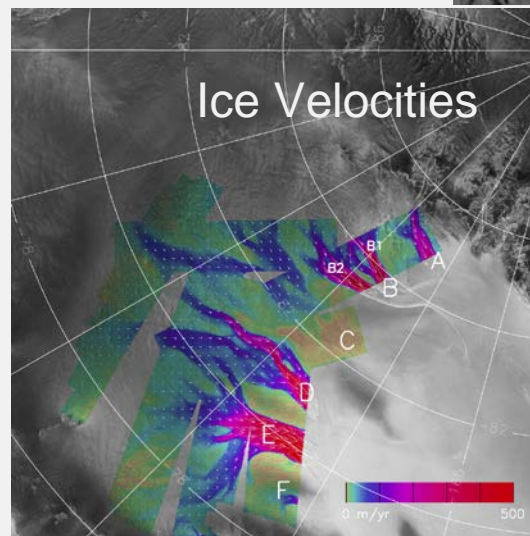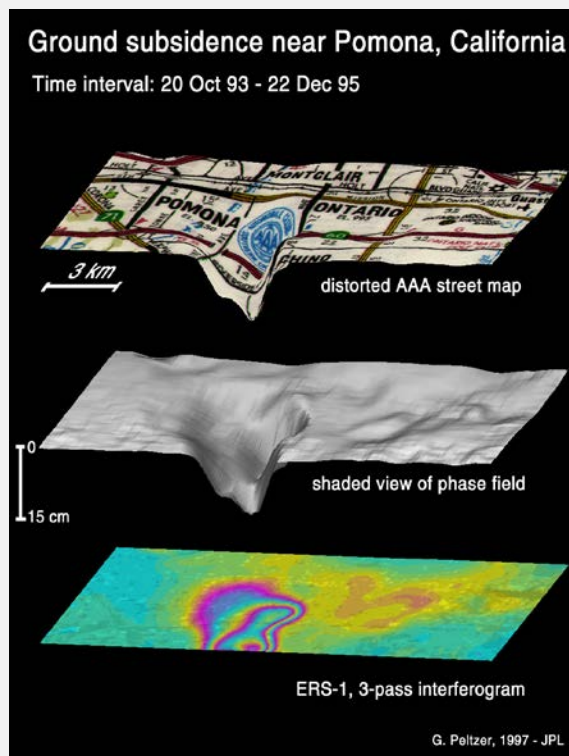
Joughin et al , 1999

# Volcanoes of the central Andes

- Map of deformation in and around volcanoes
- European ERS-1 and ERS-2 satellites (C-band)
- Some related to recent eruptions
- Others were not known to be active now
- M. Pritchard (now at Cornell)
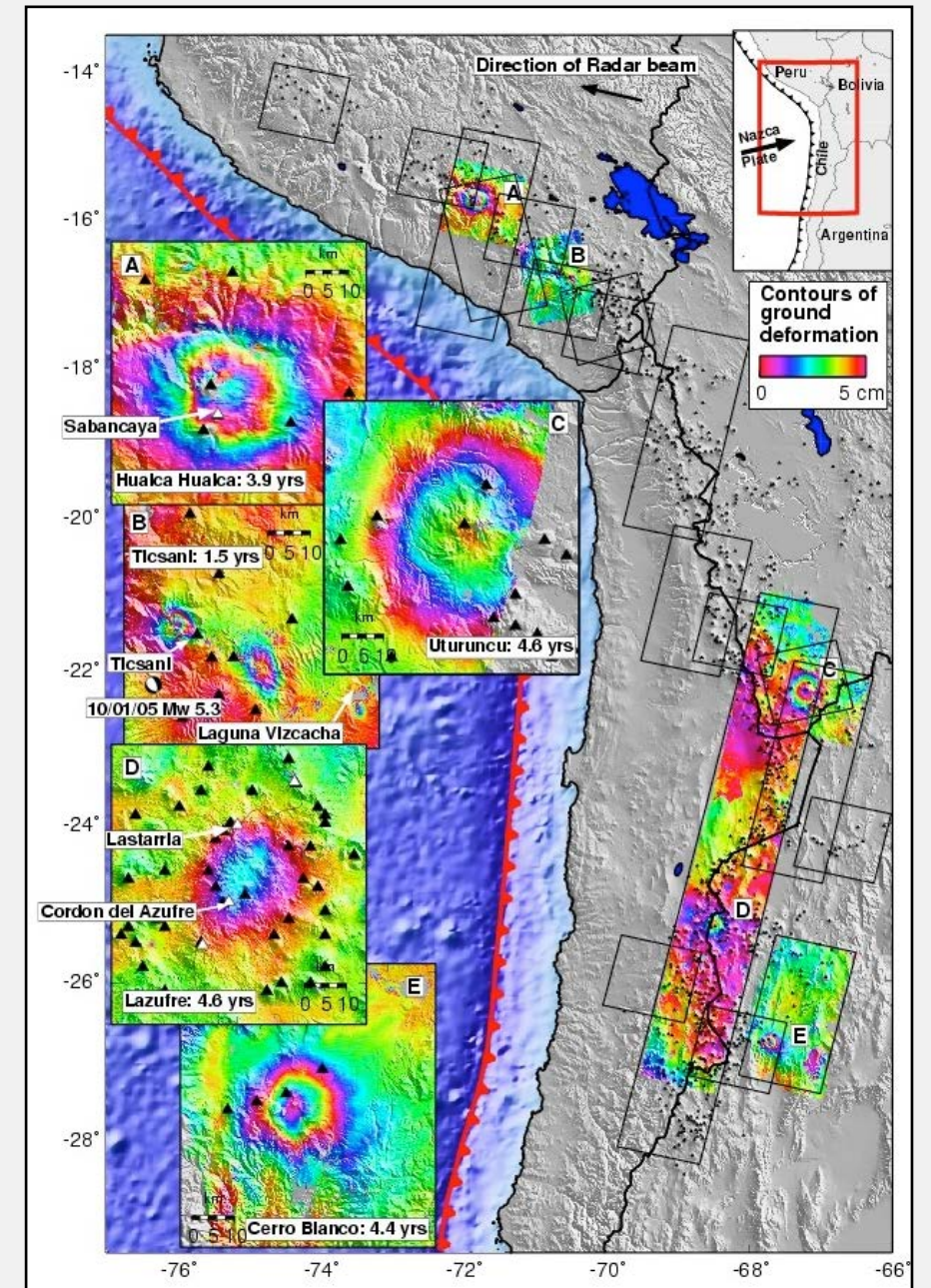
# Asal Rift Dike Injection



6 May – 28 Oct 2005; from Tim Wright, U. Leeds
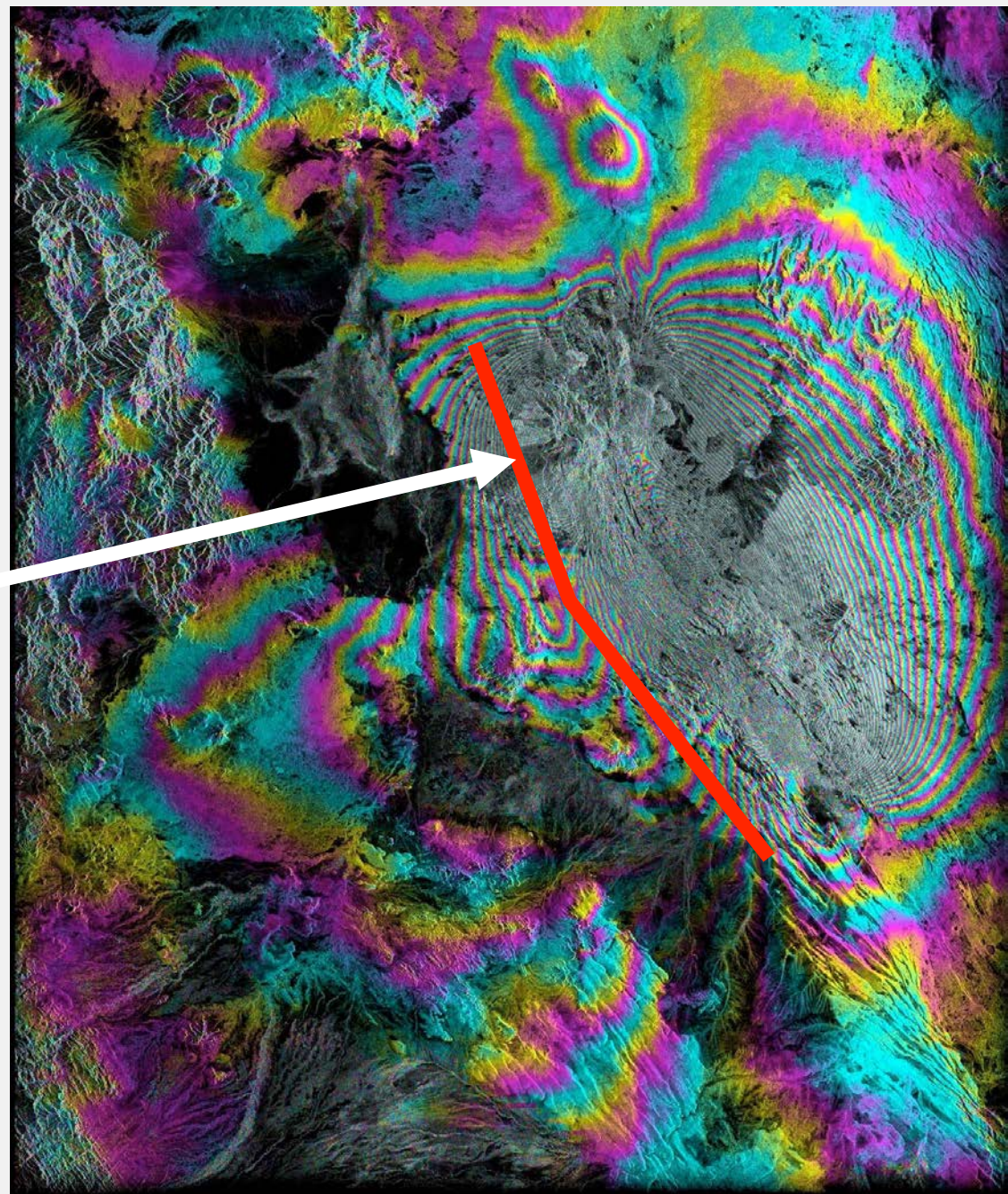
# 2015 M7.8 Gorkha Earthquake in Nepal

- ALOS-2 ScanSAR interferogram

- Descending line-of-sight (LOS) perpendicular to horizontal

- InSAR phase only sees vertical component

- High Himalayas dropped down as much as 1.2 m

- Yue, H., et al. (2016, in press), Depth varying rupture properties during the 2015 Mw 7.8 Gorkha (Nepal) earthquake, *Tectonophysics*, doi:10.1016/j.tecto.2016.07.005.
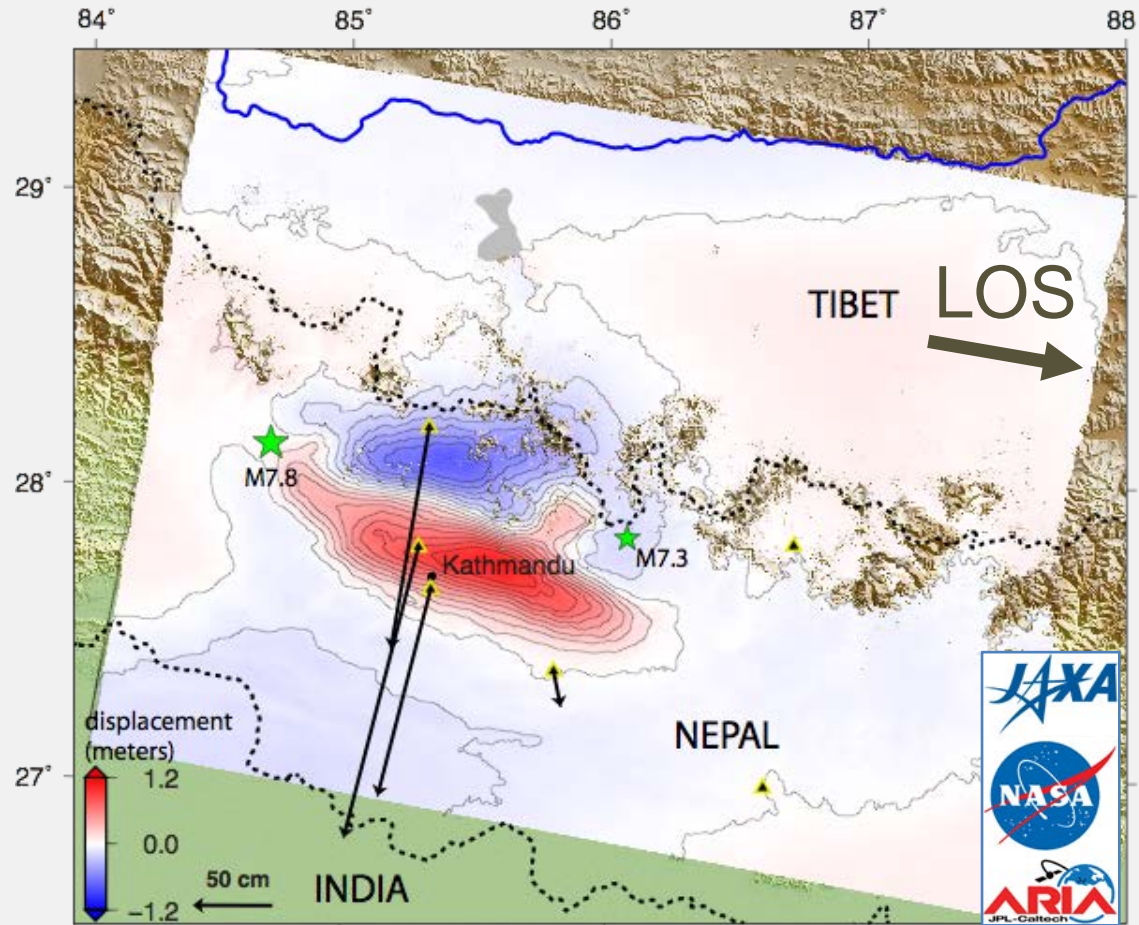


GPS data from Galetzka, J., et al. (2015), Slip pulse and resonance of the Kathmandu basin during the 2015 Gorkha earthquake, Nepal, *Science*, *349*(6252), 1091-1095

# Creep on the San Andreas Fault
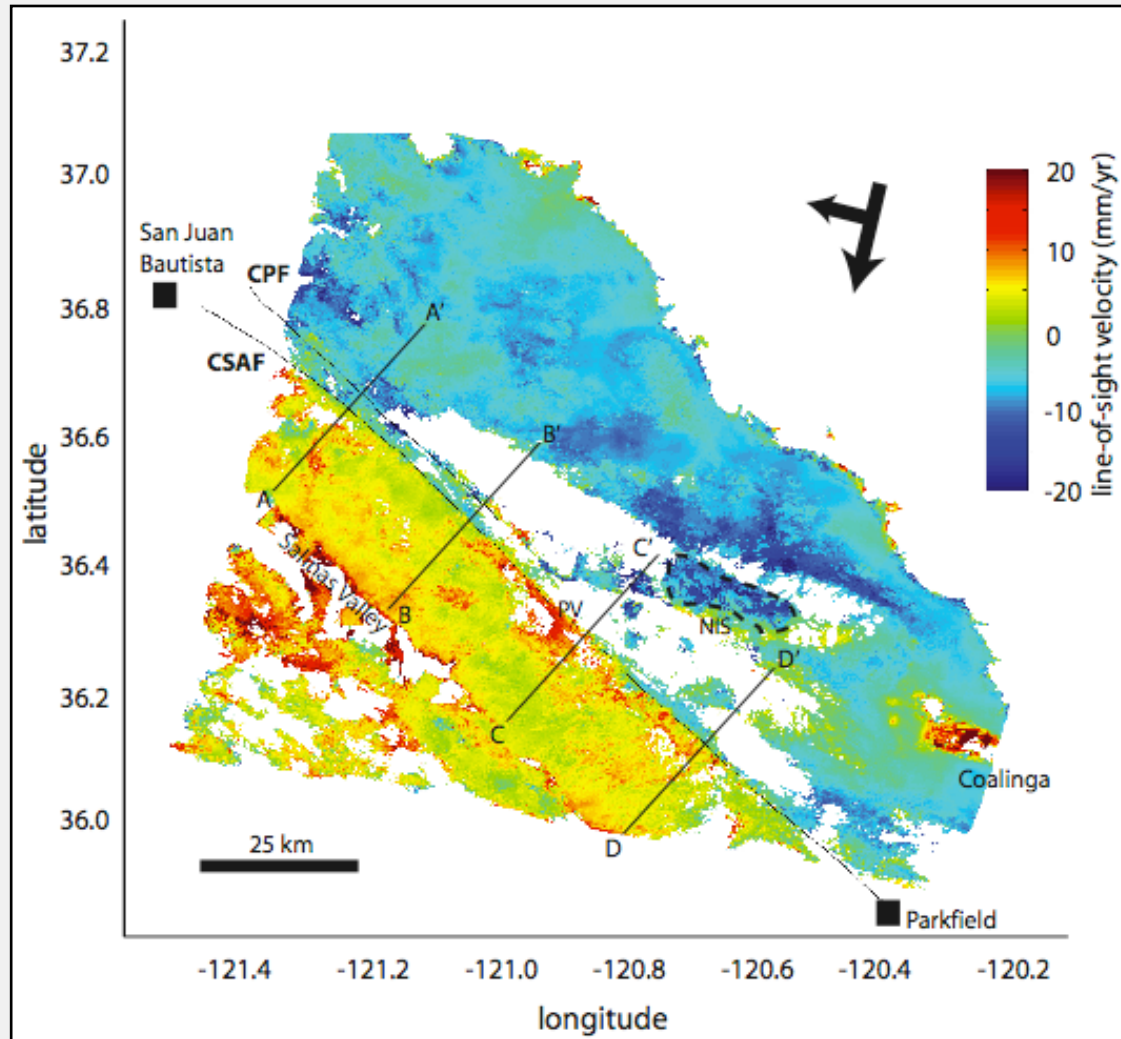


Stack of 12 ERS interferograms spanning May 1992- Jan 2001

Figures from Isabelle Ryder
UC Berkeley

# Some of InSAR's Greatest Hits

**The Ups and downs of Las Vegas (From Groundwater Pumping)**


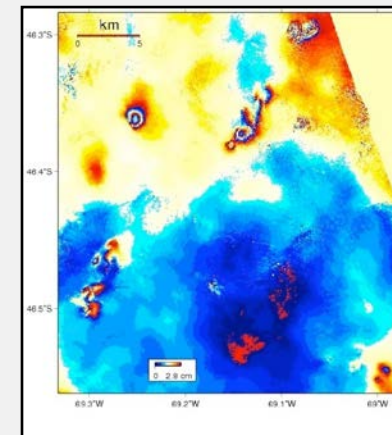
From: Amelung et al., 2000
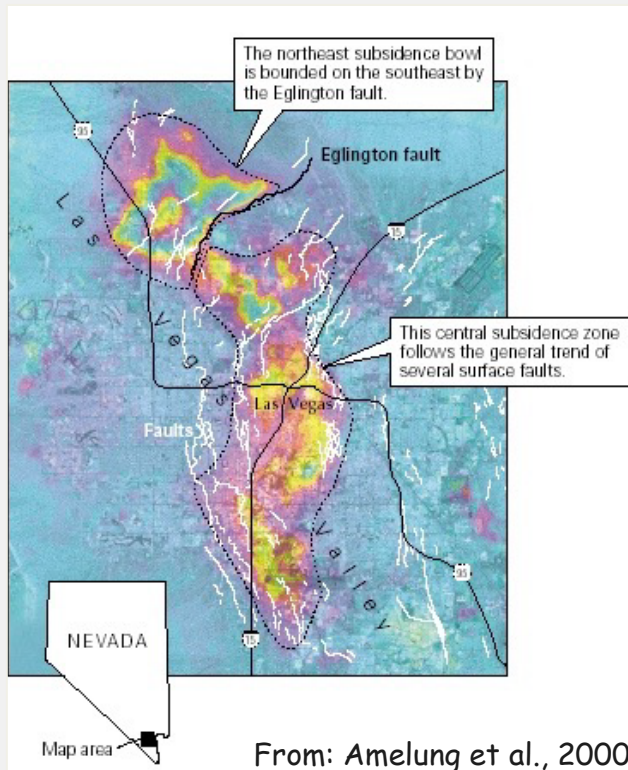
**Antarctica ice stream velocities from InSAR/feature tracking**
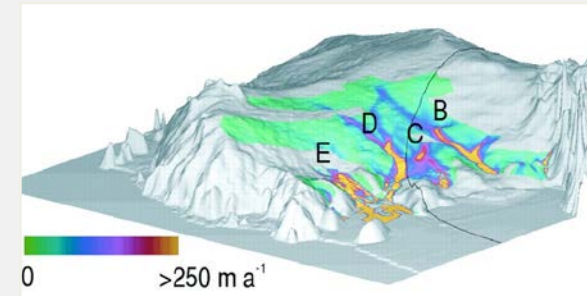


From: Bamber et al., 2000

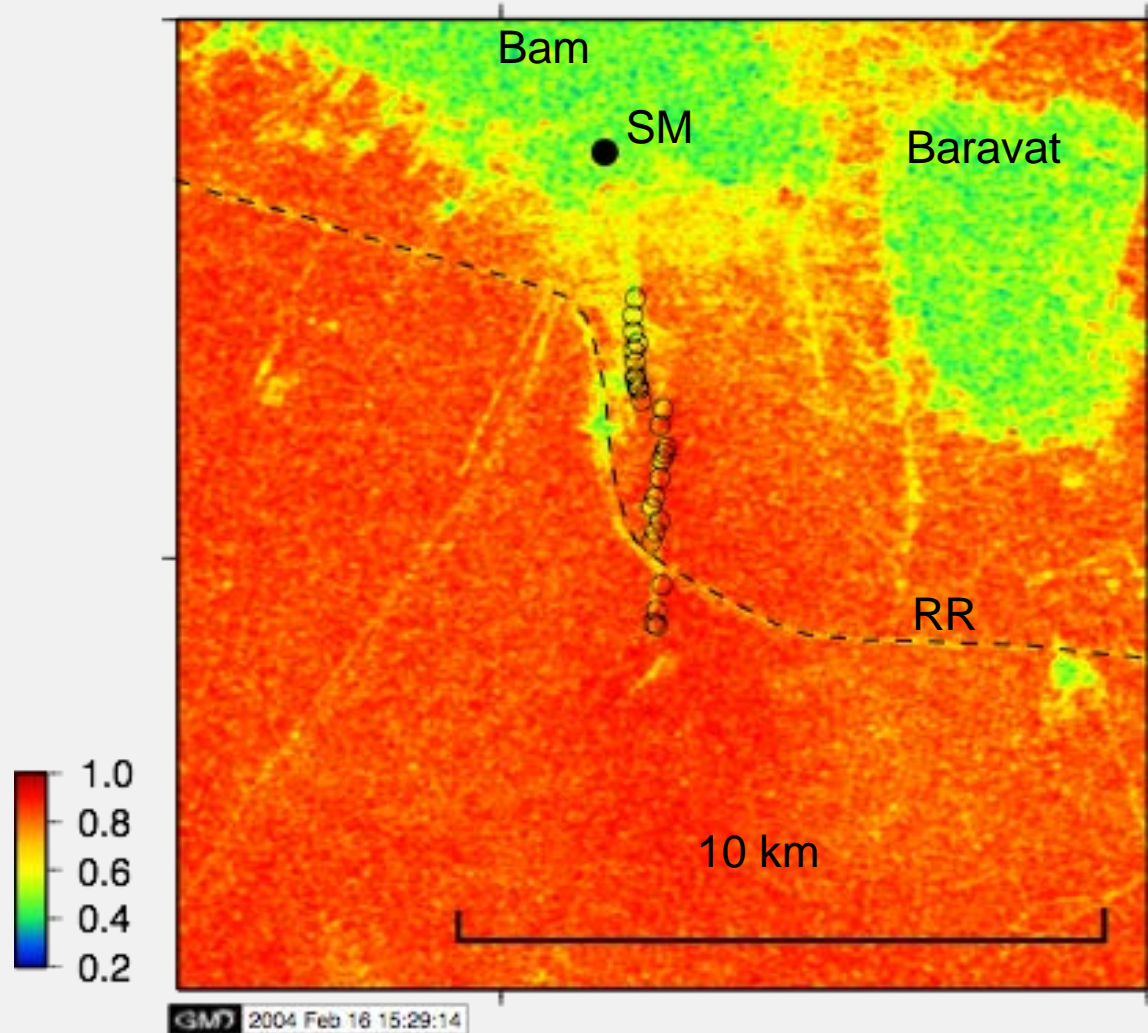Enhanced oil recovery detected in the San Jorge Basin, Argentina

Envisat interferogram spans 2004-2006

# Decorrelation shows surface ruptures

**2003 M6.5 Bam earthquake in Iran**



35 days
2003/12/3 –
2004/1/7

Envisat

Descending track

Bperp 580 m

Fielding, E. J., M. Talebian, P. A. Rosen, H. Nazari, J. A. Jackson, M. Ghorashi, and R. Walker (2005), Surface ruptures and building damage of the 2003 Bam, Iran, earthquake mapped by satellite synthetic aperture radar interferometric correlation, *J. Geophys. Res.*, *110*(B3), B03302, doi:10.1029/2004JB003299.
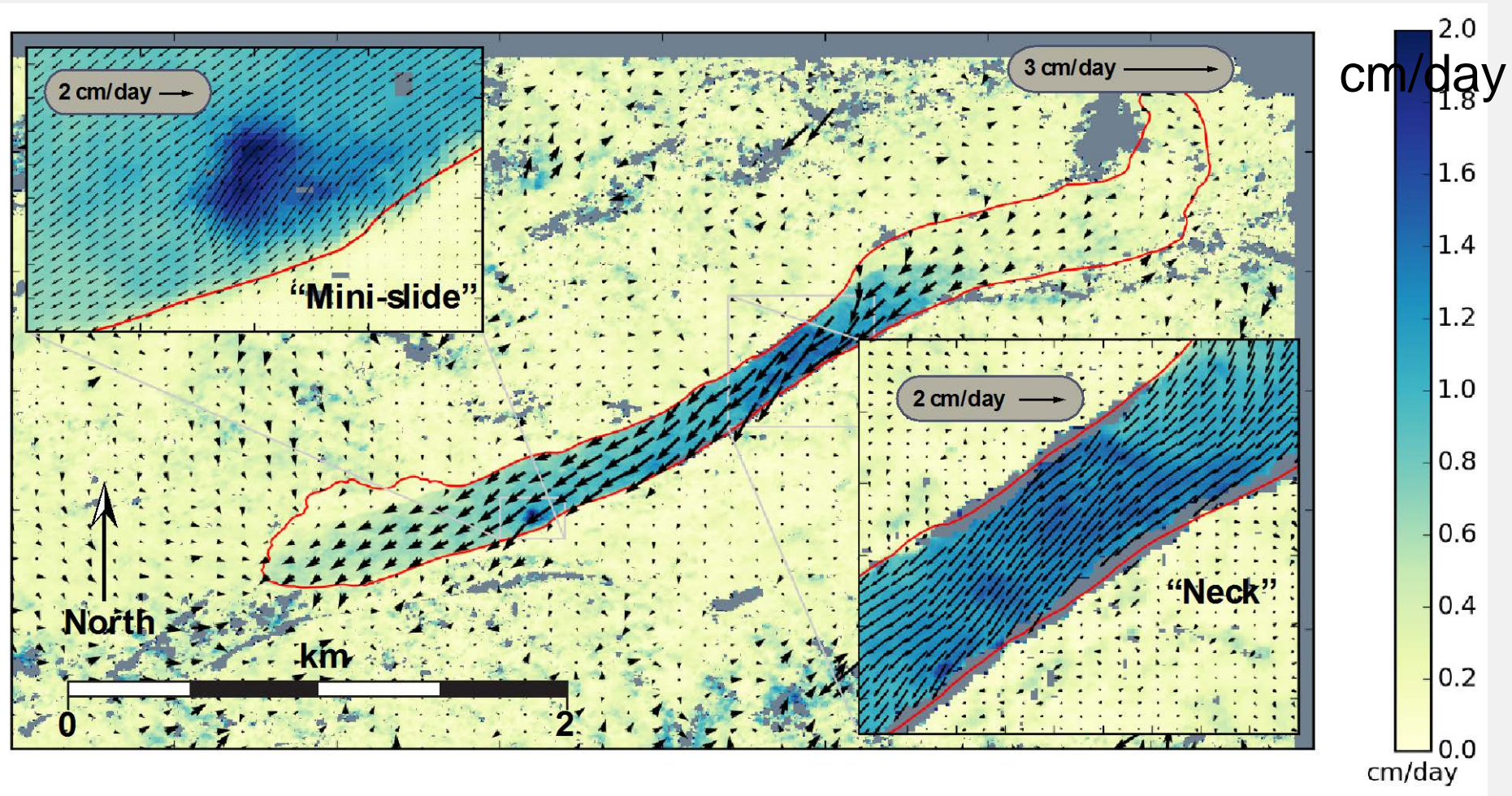
# Correlation change
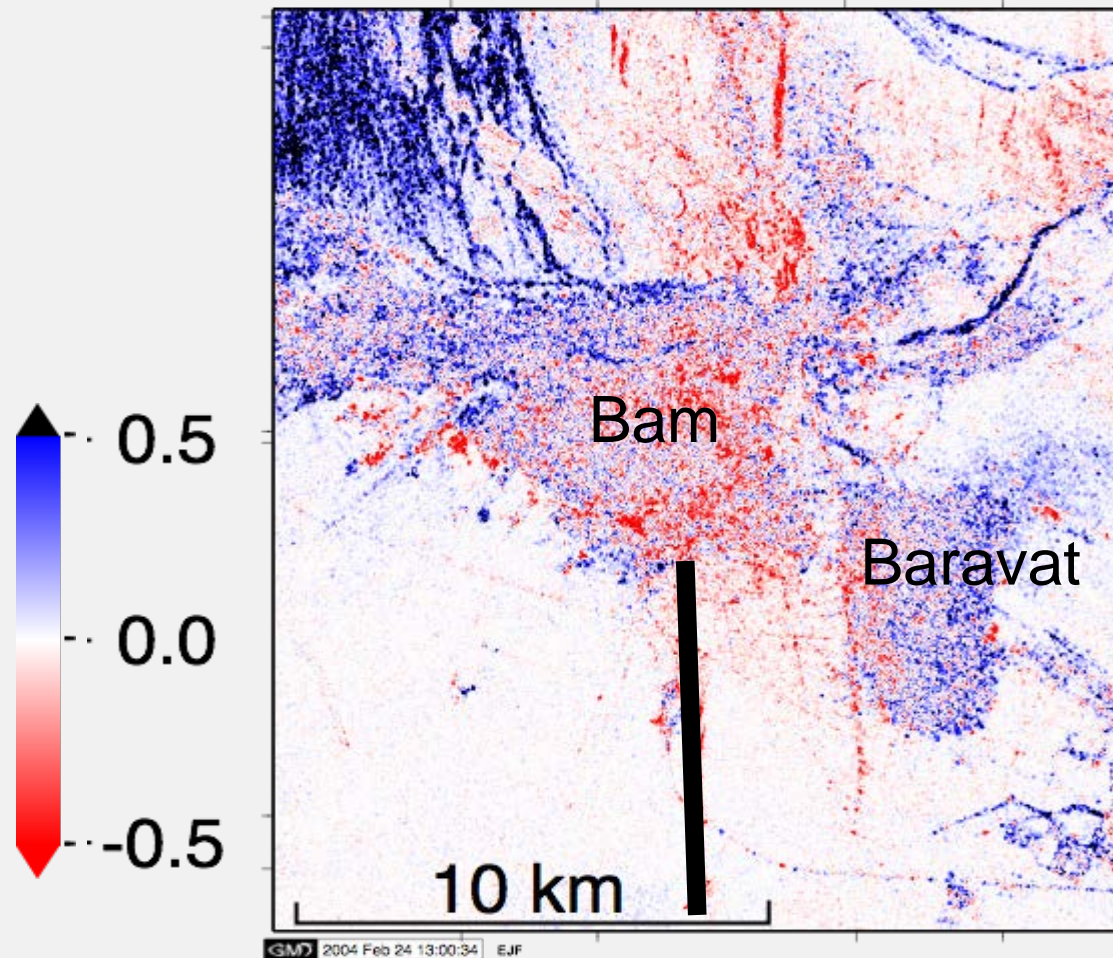


co-seismic correlation
minus pre-seismic
correlation

red is
co-seismic
decorrelation

# Landslide Motion

- Combination of four NASA UAVSAR InSAR flight lines



Delbridge, B. G., R. Bürgmann, E. Fielding, S. Hensley, and W. H. Schulz (2016), Three-dimensional surface deformation derived from airborne interferometric UAVSAR: Application to the Slumgullion Landslide, J. Geophys. Res. Solid Earth, 121(5), 3951--3977, doi:10.1002/2015JB012559.
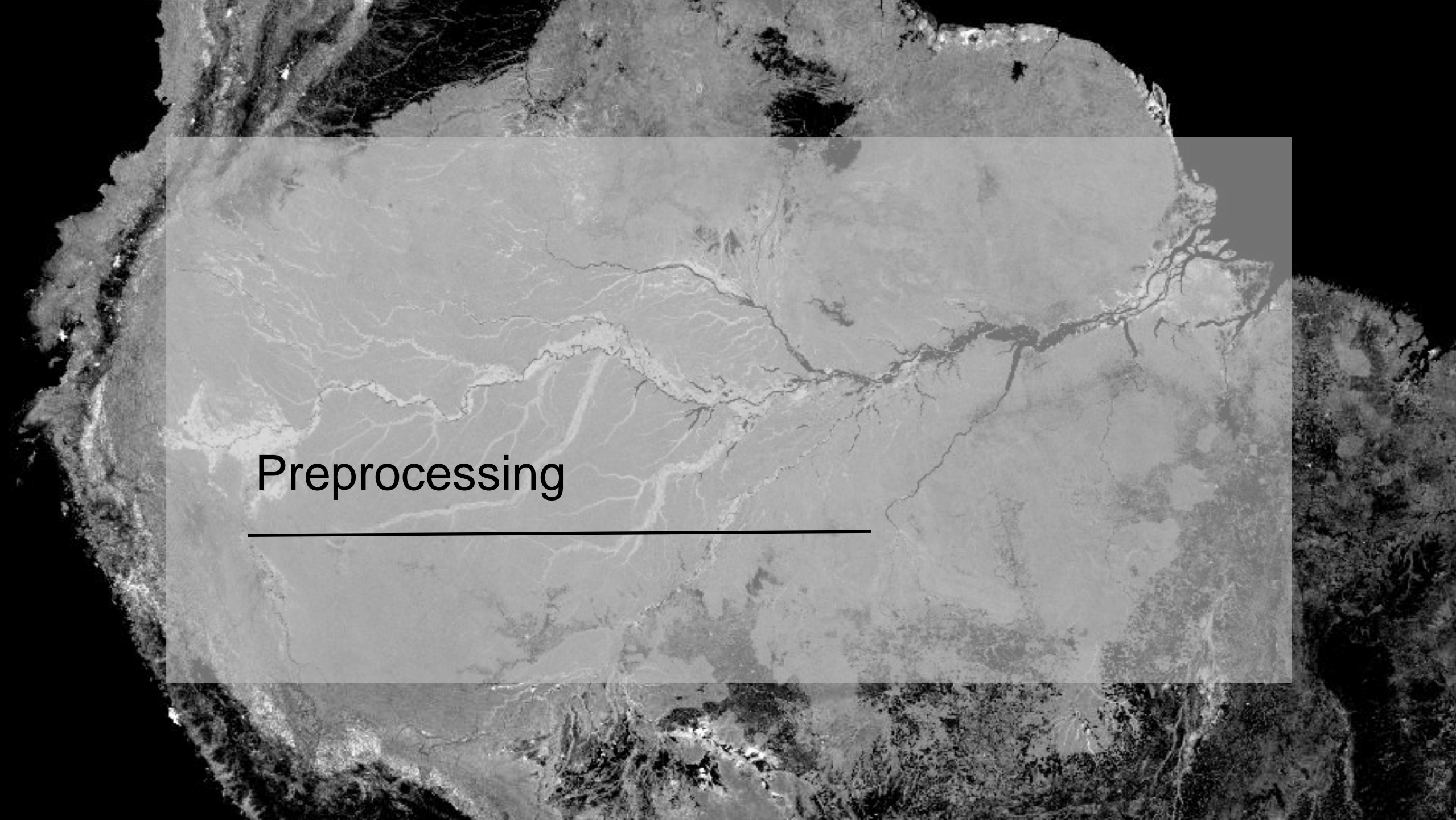
# NASA-ISRO SAR Mission (NISAR)

- High spatial resolution with frequent revisit time

- Earliest baseline launch date: 2021

- Dual frequency L- and S-band SAR
  - L-band SAR from NASA and S-band SAR from ISRO

- 3 years science operations (5+ years consumables)

- All science data will be made available free and open

- https://nisar.jpl.nasa.gov

- Slide Courtesy of Paul Rosen (JPL)

| NISAR Characteristic: | Would Enable: |
|---|---|
| L-band (24 cm wavelength) | Low temporal decorrelation and foliage penetration |
| S-band (12 cm wavelength) | Sensitivity to light vegetation |
| SweepSAR technique with Imaging Swath >240 km | Global data collection |
| Polarimetry (Single/Dual/Quad) | Surface characterization and biomass estimation |
| 12-day exact repeat | Rapid Sampling |
| 3-10 meters mode-dependent SAR resolution | Small-scale observations |
| 3 years since operations (5 years consumables) | Time-series analysis |
| Pointing control < 273 arcseconds | Deformation interferometry |
| Orbit control < 500 meters | Deformation interferometry |
| >30% observation duty cycle | Complete land/ice coverage |
| Left/Right pointing capability | Polar coverage, North and South |
| Noise Equivalent Sigma Zero ≤ -23 db | Surface characterization of smooth surfaces |

# Accessing, Opening, and Displaying SAR Interferometry Data

# Preprocessing